



THE UNIVERSITY OF  
**SYDNEY**

SCHOOL OF AEROSPACE MECHANICAL AND MECHATRONIC ENGINEERING

AERO3760: SPACE ENGINEERING 2

---

## Group E: SnapSat

### Data Package Document 1 Critical Design Review

---

21 AUGUST 2015

Name and Email	Role and Responsibility
James Allworth   312073038 jall8741@uni.sydney.edu.au	<i>Attitude Determination and Control System</i> TASKS
Thomas Forbutt   312101058 tfor8012@uni.sydney.edu.au	<i>Communications and Data Handling</i> TASKS
Oscar McNulty   312106130 omcn3220@uni.sydney.edu.au	<i>Structural Design and Development</i> TASKS
Penelope Player   312106718 ppla7388@uni.sydney.edu.au	<i>On-board Computer and Power System</i> TASKS
Nikita Sardesai   312088205 nsar2497@uni.sydney.edu.au	<i>Thermal System Design and Payload</i> TASKS

Table 0.1: caption

# Contents

<b>1 System Overview . . . . .</b>	<b>3</b>
<b>2 Payload Design . . . . .</b>	<b>4</b>
<b>3 Structural Subsystem . . . . .</b>	<b>5</b>
<b>4 Attitude Determination and Control Subsystem . . . . .</b>	<b>6</b>
4.1 Selection of Magnetorquers . . . . .	6
4.2 Design of Magnetorquer . . . . .	6
4.3 Construction of Magnetorquers . . . . .	7
4.4 Magnetorquer Control System . . . . .	8
<b>5 Electrical Power Subsystem . . . . .</b>	<b>9</b>
<b>6 On-Board Computer and On-board Data Handling Subsystem . . . . .</b>	<b>10</b>
<b>7 Communications Subsystem . . . . .</b>	<b>11</b>
<b>8 Thermal Control Subsystem . . . . .</b>	<b>12</b>
8.1 The Three Modes of Heat Transfer . . . . .	12
8.1.1 Convection . . . . .	13
8.1.2 Conduction . . . . .	13
8.1.3 Radiation . . . . .	13
8.2 Total Incoming Radiation . . . . .	13
8.2.1 View Factors . . . . .	14
8.3 Spacecraft Thermal Environment . . . . .	15
8.3.1 Solar Radiation . . . . .	15
8.3.2 Earth Infrared Radiation . . . . .	16
8.3.3 Earth Albedo . . . . .	16
8.3.4 Total Incoming Radiation Per Panel . . . . .	17

# List of Figures

4.1 Magnetorquer Construction Set Up . . . . .	7
4.2 Completed Magnetorquer . . . . .	8
4.3 Simulink Model of Control System . . . . .	8
8.1 Incoming thermal radiation on the satellite . . . . .	12
8.2 Radiation incoming onto the satellite as it orbits . . . . .	14
8.3 Representation of Satellite Orbit . . . . .	15
8.4 Solar radiation falling on each panel . . . . .	16
8.5 Reflected albedo falling on each panel . . . . .	17
8.6 Total radiation falling upon panel 2 . . . . .	17

# List of Tables

0.1 caption . . . . .	1
-----------------------	---

4.1 Predicted Data for the Magnetorquers . . . . .	6
--	---

# **1 System Overview**

## **2 Payload Design**

### **3 Structural Subsystem**

## 4 Attitude Determination and Control Subsystem

### 4.1 Selection of Magnetorquers

The SnapSat is a relatively small satellite with low mass and power considerations. After extensive literature review it was determined that given the mass and power consideration of the SnapSat, magnetorquers would provide a better controls system than

### 4.2 Design of Magnetorquer

The torque on the satellite produced by the magnetorquer is given by cross product of the magnetic dipole of the magnetorquer and the earth's magnetic field strength:

$$T = M \times B$$

It is impossible to change the earth's magnetic field strength which is approximately  $3 \times 10^{-6}$  Tesla. Thus in order to maximise the torque on the satellite the magnetic dipole must be maximised. The magnetic dipole for the magnetorquer is given by the following equation:

$$M = N \cdot I \cdot A$$

Thus the magnetic dipole is dependent on the number of turns in the coil, the current through the wire and the area of the coil. Initially it seems like a simple problem where the dipole will simply increase with the number of turns if the current and area are held constant. However, this view does not take into account the resistance that increases with the length of wire, which given the fixed voltage will limit the current. Due to cost restrictions, only 0.18mm round copper wire was available for use, which had a resistance per metre ( $R_m$ ) of 0.646 ohms. The following equations were then combined with the magnetic dipole equation in order to optimise the number of turns required:

$$I = \frac{V}{R}$$

$$R = N \cdot Perimeter \cdot R_m$$

$$P = V \cdot I$$

When combined the following equation was determined:

$$1 = \frac{4 \cdot M \cdot R_m}{V \cdot A}$$

Thus since resistance per metre and voltage are constant, and perimeter is dependent on area, the magnetic dipole becomes constant for a given area. Due to the restrictions in the lab only two sizes were available for the magnetorquers. The larger size was selected with side lengths of 0.073m as when the smaller size was modelled, the current draw was too high causing a higher level of power to be used. Thus given this fixed area, the maximum magnetic dipole was determined to be  $0.14Am^2$ . Using this maximum dipole as the basis, the other characteristics of the magnetorquer were determined and can be viewed in the table below.

Table 4.1: Predicted Data for the Magnetorquers

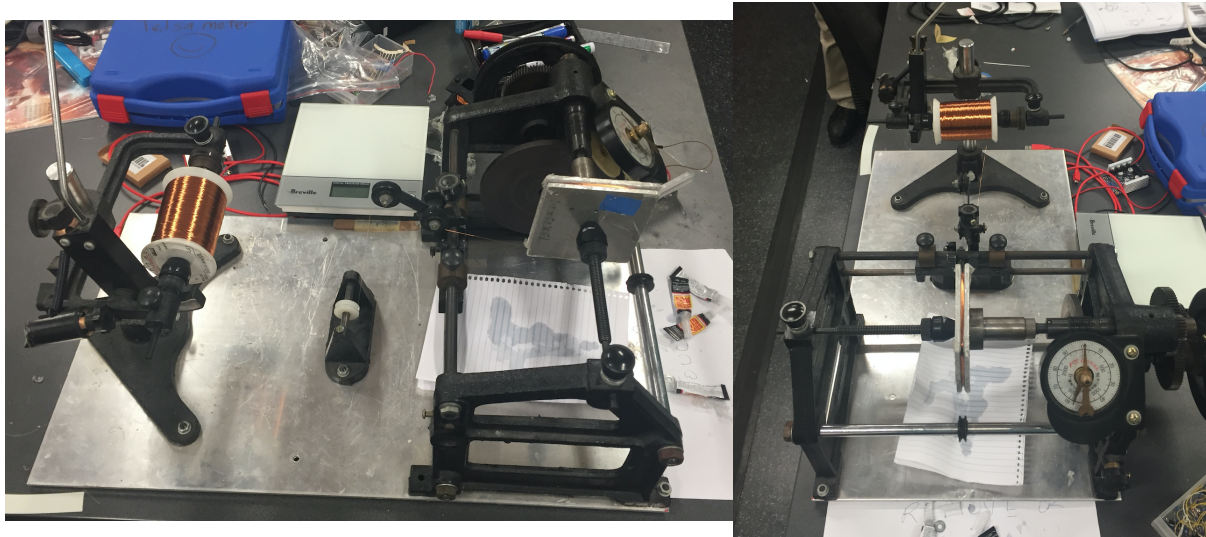
Magnetic Dipole	Number of Turns	Current	Area	Voltage	Resistance	Power Required
$0.14Am^2$	132	0.2A	$0.005329m^2$	5V	24.9Ω	1W

### 4.3 Construction of Magnetorquers

As mentioned previously the Magnetorquers were built in house using equipment provided in the space lab. The following procedure was applied to make each magnetorquer:

1. The metal structural mould for the magnetorquer was unscrewed and sticky tape was applied to areas that were likely to come into contact with glue.
2. The mould was placed in the winder and the copper wire was set up as shown in the photographs below.

Figure 4.1: Magnetorquer Construction Set Up



3. The wire at the very beginning of the coil was taped to the side of the mould to keep it separate from the coil so that it can be connected to the PCB.
4. In order to measure the number of turns, the counter on the winder was set to zero.
5. Twenty turns were completed and then a layer of super glue was added to the coiled wire on all four sides in order using a thin brush.
6. Step 4 was repeated until the required number of turns was reached at which point another layer of glue was added to each side of the coil.
7. The copper wire was cut and the wire at the very end of the coil was not stuck to the main coil in order to provide a connection between the PCB and the magnetorquer.
8. The glue was allowed to set for 10 mins and then the coil was carefully removed from the mould with the aid of the sticky tape.
9. Once completed the ends of coil were carefully scraped with sandpaper in order to remove the protective coating and allow current to be passed through.
10. The coil was tested by attaching it to a battery and using a compass to determine whether a magnetic field was being produced.

11. An Ohmmeter was used to determine the resistance through the coil.

After testing both magnetorquers were found to have a slightly higher resistance than predicted with the first magnetorquer reading a resistance of  $27.2\Omega$  and the second magnetorquer reading  $28.1\Omega$ . This is roughly a 10% increase on the predicted value of  $24.9\Omega$  and is most likely caused by the effect of the super glue which was not taken into consideration in the original calculations. This will result in the magnetorquers using a slightly lower current as voltage is constant and have a lower maximum dipole value. These values were calculated to be  $0.138 Am^2$  and  $0.137 Am^2$  for magnetorquers 1 and 2 respectively. The image below depicts magnetorquer 1 just after construction.

Figure 4.2: Completed Magnetorquer



#### 4.4 Magnetorquer Control System

The dynamic model for the magnetorquer control system was produced by three fundamental equations:

$$T = N \cdot I \cdot A \cdot B \cdot \sin(\theta)$$

$$V = I \cdot R$$

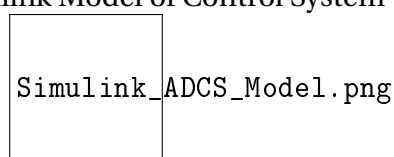
$$T = J \cdot \ddot{\theta}$$

By combining these three equations and using a Laplace transform the following dynamic model was determined:

$$\frac{\theta(s)}{V(s)} = \frac{N \cdot A \cdot B}{J \cdot R \cdot s^2(s^2 + 1)}$$

Thus using this function the following Simulink model was produced to determine the expected response of the satellite given certain inputs.

Figure 4.3: Simulink Model of Control System



## **5 Electrical Power Subsystem**

## **6 On-Board Computer and On-board Data Handling Subsystem**

## **7 Communications Subsystem**

## 8 Thermal Control Subsystem

The method of developing thermal control used for SnapSat considers the following simplified model of the satellite. The main body is idealised as a system dissipating heat (located at the centre of the CubeSat) to the boundary located on the face of the CubeSat. This boundary is exposed to the outer environment. Energy conservation laws require that in steady state, the heat dissipated by the internal electronics is equal to that transferred to the boundary. Thus, the heat from internal dissipation added to the heat adsorbed from the outside is equal to the heat rejected to space. The general governing equation is

$$Q_{1 \rightarrow 2} = K_{1 \rightarrow 2}(T_a - T_2) \quad (8.1)$$

Where  $Q$  = heat exchange (Watts)

$K$  = proportionality factor constant (Watts/Kelvin)

$T$  = temperature of bodies (Kelvin)

between bodies 1 and 2. Additionally, the heat radiated from a blackbody surface of temperature  $T$  is given by

$$Q_r = KT^4 \quad (8.2)$$

Where the proportionality factor depends on physical constants, the material properties, surface conditions and geometry. A schematic of the incoming thermal radiation on the CubeSat in Low-Earth Orbit (LEO) is shown below.

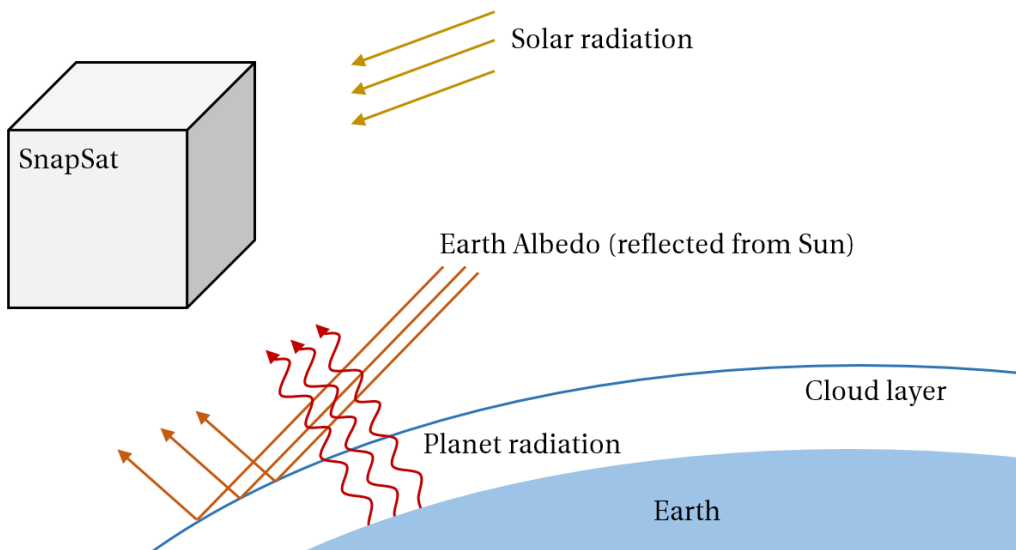


Figure 8.1: Incoming thermal radiation on the satellite

### 8.1 The Three Modes of Heat Transfer

The first law of thermodynamics states that the internal energy change on a system is equal to the amount of heat added subtracted by the amount of work done. The work done by the satellite on its environment is zero in our case, so the change in energy becomes

$$\frac{dU}{dt} = Q = A \rho c_p \frac{dT}{dt} dx$$

Where  $Q$  = heat added (Watts)  
 $A$  = cross-sectional area ( $\text{m}^2$ )  
 $\rho$  = density of material ( $\text{kg}/\text{m}^3$ )  
 $c_p$  = specific heat capacity ( $\text{J}/\text{kg K}$ )  
 $T$  = temperature (K)  
 $dx$  = incremental length (m)

Is is dependent on the physical and geometric properties of the satellite and the change in temperature. The total heat balance for the satellite is then given by the heat flux entering the system minus the flux leaving the system. These are characterised by the modes of heat transfer below.

### 8.1.1 Convection

Convection is the heat transfer between a solid surface and flowing fluid. This is of importance during mission launch, however does not apply in a space environment. Convection considerations were ignored for this design.

### 8.1.2 Conduction

Thermal energy transfer within a material due to vibrating atoms - for example if the material is heated in one location, conduction is the method by which it spreads to the rest of the material. This is most important for on-board electronics, the rate of heat transfer is given by

$$Q_{conduction} = \frac{kA}{\Delta x}(T_1 - T_2)$$

which is the same as equation 8.1. The heat transfer depends on the area of the satellite normal to the direction of heat transfer  $A$ , the thermal conductivity  $k$  and the temperature differential  $T$ .

### 8.1.3 Radiation

Perhaps the most complex form of heat transfer is radiation, where all bodies above 0K emit and absorb electromagnetic energy. We consider each body as a perfect emitter (black body) and integrate the emitted energy across all wavelengths, this gives

$$E_{bb} = \epsilon\sigma T^4 \quad (8.3)$$

measured in  $\text{Watts}/\text{m}^2$ . This is the same as equation 8.2, where  $\sigma$  is the Stefan-Boltzmann constant. In this case, the emissivity  $\epsilon$  has been added to account for the fact that the surfaces are not perfect black bodies.

## 8.2 Total Incoming Radiation

The total radiation incoming onto the satellite as it orbits is defined in figure 8.2 below. This assumes that the satellite is in full view of the sun 65% of the time in each orbit.

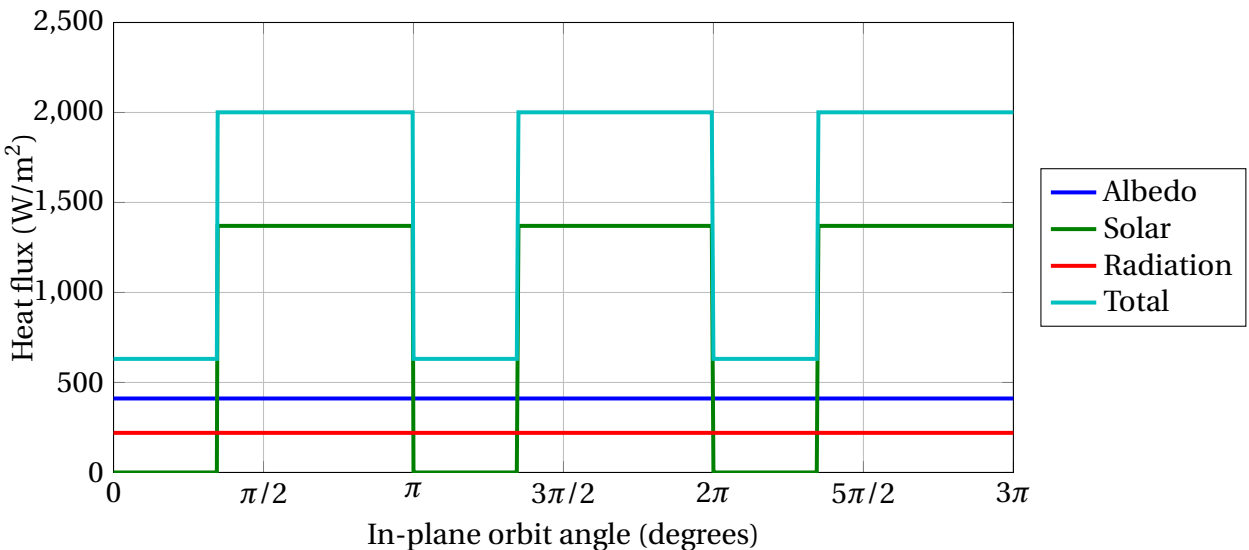


Figure 8.2: Radiation incoming onto the satellite as it orbits

Whilst this is the incoming radiation on the satellite as a whole, it is not indicative of the amount of radiation received by each side of the satellite. As the spacecraft is attitude controlled, the lower side will be facing the Earth always and only receive solar radiation for a short period of time. The amount of solar radiation (and even Earth IR radiation) received depends on the projected area that the radiation falls upon. Corrections are found using the view factor of each side of the satellite.

### 8.2.1 View Factors

The view factor of each side of the satellite allows for the calculation of the effect of the incoming radiation. The calculation takes into account the projected amount of heat flux on each side. The view factor is of importance when considering the radiation effect of Earth's infrared and albedo. The view factor indicates the area of the panel that radiation falls upon. The formulae to obtain the view factors for each panel is

$$F_{i \rightarrow j} = \frac{1}{A_i} \int_{A_i} \int_{A_j} \frac{\cos\theta_1 \cos\theta_j}{\pi S^2} \quad (8.4)$$

Where  $S$  is the shape factor. Whilst this a complex equation (especially for complex geometries), the view factors for a simple cubesat orbiting a sphere (Earth) are

$$V_F = \frac{\cos\gamma}{H} \quad (8.5)$$

If the panel is facing towards Earth such that the whole surface can be 'seen' by the panel. However if the panel is not facing the Earth

$$V_F = 0 \quad (8.6)$$

If the panel is oriented in such a way that it is only partially oriented to see the Earth then

$$V_F = \frac{1}{2} - \frac{1}{\pi} \sin^{-1} \left( \frac{(H^2 - 1)^{1/2}}{H \sin \gamma} \right) + \frac{1}{\pi H^2} \cos \gamma \cos^{-1}(-(H^2 - 1)^{1/2} \cot \gamma) \quad (8.7)$$

$$- \frac{1}{\pi H^2} (H^2 - 1)^{1/2} \times (1 - H^2 \cos^2 \gamma)^{1/2} \quad (8.8)$$

Where  $\gamma$  is the angle between the normal to the Earth's surface (or normal to the projected disk that the satellite panel sees) and the normal to the panel. [1]

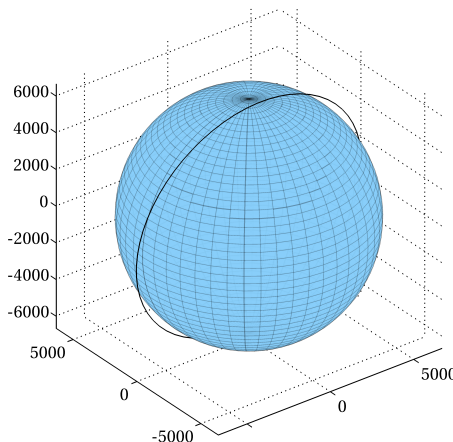


Figure 8.3: Representation of Satellite Orbit

### 8.3 Spacecraft Thermal Environment

As shown in figure 8.1, the spacecraft is subject to the following heating mediums: solar radiation, Earth infra-red and Earth albedo. The amount of radiation falling upon each panel is a function of the surface absorptivity and the view factor of the panel. The panel naming convention for this section is shown below.

#### 8.3.1 Solar Radiation

The incoming solar radiation on the satellite is given by

$$Q_{solar} = Q_{sun} \alpha \cos \phi \quad (8.9)$$

Where  $Q_{sun} = 1350$  solar heat flux ( $\text{W/m}^2$ )

$\alpha$  = panel surface absorptivity

$\phi$  = angle between the normal of the panel to the sun (rad)

For each of the panels, the solar radiation intensity is shown in the figure below. The skew in four of the panels is due to the  $45^\circ$  rotation of the orbit along the  $z$  Earth frame.

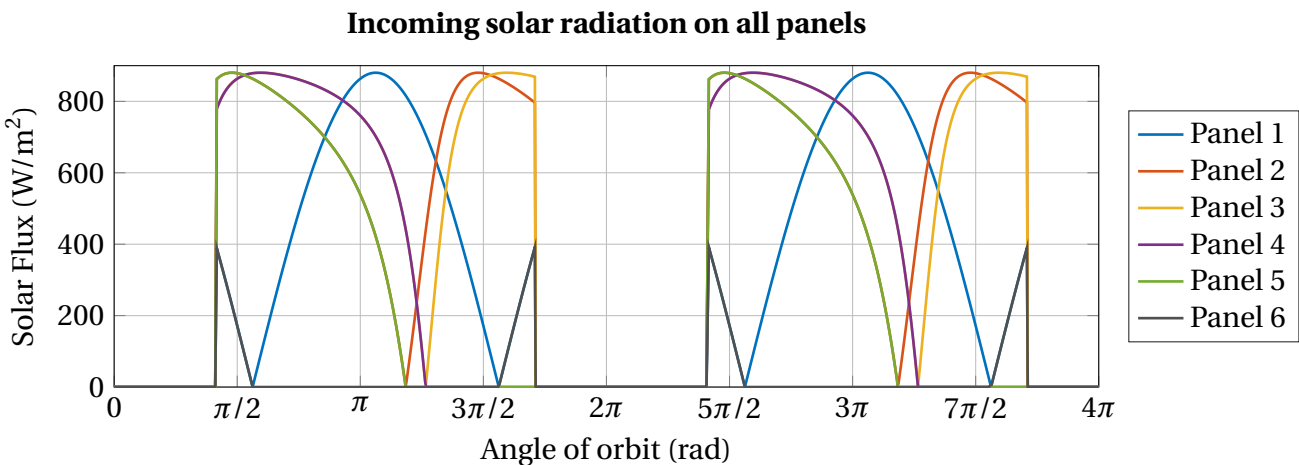


Figure 8.4: Solar radiation falling on each panel

### 8.3.2 Earth Infrared Radiation

The incoming radiation from the Earth is in the infrared band. This radiation is due to the effective temperature of the Earth and is a constant value for each panel. For this reason, the values will not be displayed on a graph. The incoming radiation varies from panel to panel depending only on the view factors as described in section 8.2.1. The value is given by

$$Q_{Earth-IR} = \sigma T_{Earth}^4 \alpha F_V \quad (8.10)$$

Where  $\sigma = 1.381 \times 10^{-23} \text{ m}^2 \text{ kg s}^{-2} \text{ K}^{-4}$  (Boltmann constant)

$T$  = effective temperature of the Earth

$\alpha$  = panel surface absorptivity

$F_V$  = panel view factor

### 8.3.3 Earth Albedo

The final source of external radiation is the Earth albedo, which is solar radiation that has been reflected off the Earth's could layer. The value as the cubesat orbits the Earth is given by

$$Q_{Earth-albedo} = Q_{sun} F_A \alpha F_V \cos\theta \quad (8.11)$$

Where  $Q_{sun} = 1350 \text{ W/m}^2$  (solar radiation)

$F_A$  = albedo view factor

$\alpha$  = panel surface absorptivity

$F_V$  = panel view factor

$\theta$  = angle between the spacecraft panel surface and the Sun (8.12)

The figure below shown the variation in albedo that three panels see throughout the orbit. Since each panel is not double sided, the plot cycles between two opposite panels. For instance, the orange line shown the albedo incoming on both panels 2 and 5 (the panel on the opposite side). Half of the cycle representing each panel.

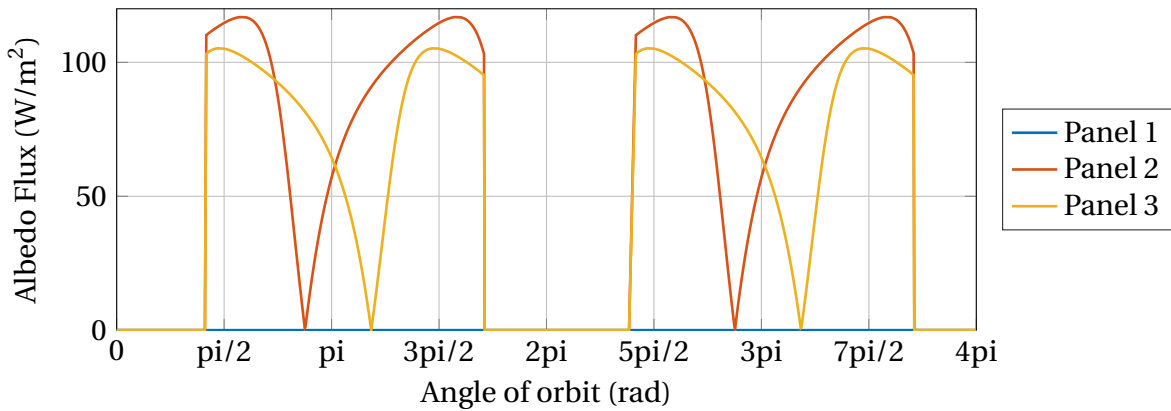


Figure 8.5: Reflected albedo falling on each panel

### 8.3.4 Total Incoming Radiation Per Panel

For illustration purposes, figure 8.6 shows the total incoming radiation on panel 2. This calculation was performed for all six panels.

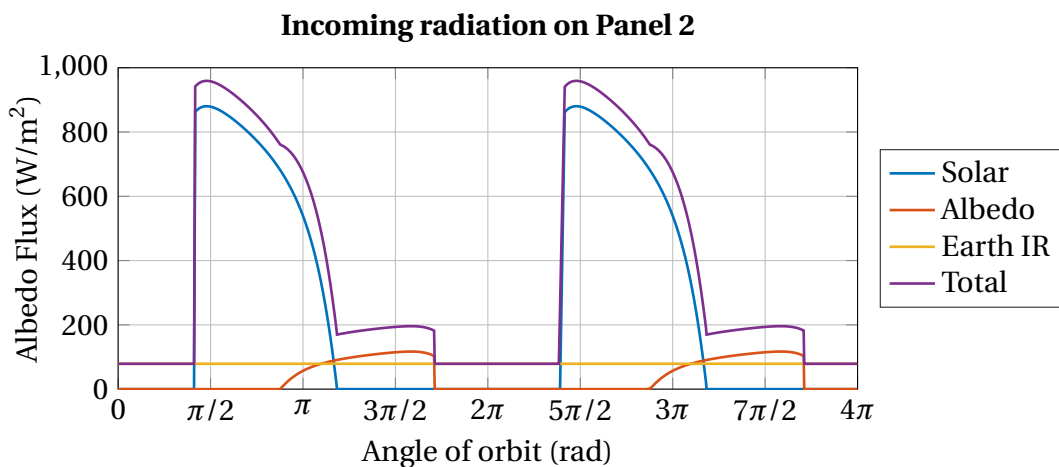


Figure 8.6: Total radiation falling upon panel 2

## References

- [1] H. Heidt, J. Puig-Suari, A. Moore, S. Nakasuka, and R. Twiggs, “Cubesat: A new generation of picosatellite for education and industry low-cost space experimentation,” 2000.